CrossMark

Electrochemical dealloying using pulsed voltage waveforms and its application for supercapacitor electrodes

Jie Zhang [a,b,c], Yawen Zhan [a,b,c], Haidong Bian [a,c], Zhe Li [a,b,c], Chun-Kwan Tsang [a,b,c], Chris Lee [a,b,c], Hua Cheng [a,b,c], Shiwei Shu [c], Yang Yang Li [a,c,d,*], Jian Lu [b,e]

[a] Center of Super-Diamond and Advanced Films (COSDAF), City University of Hong Kong, 83 Tat Chee Avenue, Kowloon, Hong Kong
[b] Department of Mechanical and Biomedical Engineering, City University of Hong Kong, 83 Tat Chee Avenue, Kowloon, Hong Kong
[c] Department of Physics and Materials Science, City University of Hong Kong, 83 Tat Chee Avenue, Kowloon, Hong Kong
[d] City University of Hong Kong Shenzhen Research Institute, 8 Yuexing 1st Road, Shenzhen Hi-Tech Industrial Park, Nanshan District, Shenzhen, China
[e] Centre for Advanced Structural Materials, City University of Hong Kong Shenzhen Research Institute, 8 Yuexing 1st Road, Shenzhen Hi-Tech Industrial Park, Nanshan District, Shenzhen, China

HIGHLIGHTS

- A novel dealloying method using pulsed voltage waveforms is invented.
- It can lower the compositional threshold for dealloying to take place.
- It can more thoroughly remove the more reactive metal component, producing a porous metal of higher purity and higher porosity.
- It can lead to thinner ligaments.
- It can enable supercapacitor electrodes with better performance.

ARTICLE INFO

ABSTRACT

Dealloying is an important industrial technique for generating nanoporous metallic structures by selectively leaching out the more reactive metal component from an alloy material. A constant voltage is often applied to facilitate the dealloying process. Here we report the first study on dealloying with the application of a voltage waveform—specifically, pulsed voltage waveforms are applied for dealloying Ni—Cu alloys. It is found that pulsed dealloying voltage waveforms can exert a strong impact on the dealloying process by 1) significantly lowering the compositional threshold of the more reactive metal component for the dealloying reaction to take place, 2) more thoroughly removing the more reactive metal component and thus producing a porous metal of higher purity and higher porosity (volume fraction of voids), and 3) greatly affecting the morphology of the generated porous metal structure (e.g., leading to significantly thinner ligaments). The nanoporous metallic materials obtained by the pulsed voltage waveform enable supercapacitor electrodes of significantly better performance than the counterpart dealloyed with a constant voltage.

1. Introduction

Nanoporous metals are intensively investigated for their importance in a wide range of applications. Among the different techniques for fabricating nanoporous metals, dealloying is a convenient industrial technique that is commonly used to generate nanoporous metals by selectively dissolving the more reactive metal component from an alloy system, often with the aid of an electric field [1,2]. Various kinds of nanoporous metals (such as Ni, Au, Ag, Cu, and Pt) have been fabricated using the dealloying method, and applied for different applications [3–14] such as: sensors, catalysts, photonic materials, batteries, supercapacitors, etc. For example, dealloyed nanoporous Ni has lately attracted much attention for its applications in photonic materials, [10] electrochemical capacitors, [6] and electrocatalysts for hydrogen evolution [15]. Furthermore, dealloying is being applied to ever-expanding material systems. Dealloying process in intermetallics and multi-phase alloy films, [16,17] tough nanoporous metals by controlled electrochemical dealloying, [18] and selective etching of

* Corresponding author. Department of Physics and Materials Science, City University of Hong Kong, 83 Tat Chee Avenue, Kowloon, Hong Kong.
E-mail addresses: yangli@cityu.edu.hk (Y.Y. Li), jianlu@cityu.edu.hk (J. Lu).

the more noble component of an alloy, [19] have all been demonstrated. Additionally, alternating dealloying and electroplating treatments have been utilized for generating interesting porous metallic materials [20]. One of the major challenges present for the current dealloying technology is on how to control the morphology and composition of the generated porous materials. To address this challenge, the effects of different dealloying parameters, such as the etchant concentration, dealloying time, and dealloying temperature, have been studied [1,21]. Nevertheless, little attention has been paid to understand the impact of modulated anodization voltages.

Here we report the first study on dealloying with the application of a voltage waveform. To introduce our motivation, a brief introduction of the dealloying mechanism is necessary. Previous studies [22] have shown that, for binary alloys, after the more reactive metal atoms are dissolved at alloy/electrolyte interface, the more inert metal atoms at alloy/electrolyte interface undergo an atom rearrangement process and form clusters, exposing more the underlying more reactive metal atoms. The concurrent processes of chemical dissolution of the more reactive atoms and atom rearrangement of the more inert atoms allow the dissolution front to proceed and eventually penetrate throughout the whole alloy. In other words, dealloying is resulted from the dynamic interplay between atom rearrangements of the more inert metal species and the chemical etching of the more reactive metal species. Conversely, it is well-known that the chemical etching rates of metals can be easily controlled by adjusting the bias applied. Therefore, one should be able to affect the dealloying process by adjusting the bias applied. To verify this hypothesis, we dealloyed Ni–Cu alloys with pulsed voltage waveforms to generate nanoporous Ni. It was found that dealloying under a pulsed electric field provides a simple but powerful method to conveniently control the structures and compositions of the porous metals generated (e.g., more thoroughly dealloyed nanoporous metal with higher porosity and higher purity can be easily achieved) and to effectively lower the Dealloying Threshold (DT), defined here as the compositional threshold of the more reactive metals required for dealloying to take place throughout the alloy.

Moreover, this novel dealloying method proves to be particularly effective for treating alloys electrodeposited with surfactants. In order to eliminate voids and generate smoother films with finer grains, surfactants are often added into electroplating bath [23,24], however, the alloy films thus obtained are often found difficult to dealloy. Here we demonstrate that dealloying with pulsed voltage waveforms is a particularly powerful method to address this difficulty.

Finally, when used as the supercapacitor electrode materials, porous Ni fabricated using this novel dealloying method displays significantly higher specific capacitance than the conventionally dealloyed counterpart.

2. Experimental

2.1. Electrodeposition of Ni–Cu

A three-electrode cell controlled by a potentiostat (HEKA, PG 310) is used with indium tin oxide-coated glass (CSG PVTech Co., Ltd., 1.0 cm × 1.0 cm) as the working electrode, a platinum ring as the counter electrode, and a saturated calomel electrode (SCE) as the reference electrode. All the electrochemical experiments are carried out at room temperature ($\sim 20\ ^{\circ}C$) and all the potentials in this paper are reported in reference to the SCE (0.244 V vs. the standard hydrogen electrode). Electrodeposition is performed in an aqueous electrolyte: 0.5 M nickel (II) sulfamate tetrahydrate (Aldrich, 98%), 0.005 M copper (II) sulfate pentahydrate (Riedal–

Dehaën), and 0.6 M boric acid (Riedal–Dehaën). The pH value of the electrolyte is measured to be 3.83. For experiments with surfactants added in the electrolyte, 3 μg mL^{-1} of saccharin (International Laboratory USA) is added into the electrolyte. All chemicals are of analytical grade and used without further purification. The Ni–Cu films are typically deposited at −0.820 V for 130 min.

2.2. Dealloying

After the Ni–Cu film is deposited, the film is anodically etched at the room temperature in the same electrolyte used for electrodeposition. Pulse dealloying is carried out with the voltage periodically modulating between V_1 and V_2 for time durations of t_1 and t_2, respectively, for an overall period of time of $t_{dealloy}$. Unless otherwise stated, $V_1 = 0.5$ V, $t_1 = 1$ s, $V_2 = 0.06$ V, $t_2 = 5$ s, and $t_{dealloy} = 30$ min (typically the dealloying current drops to essentially zero within this period). For comparison, dealloying is also performed at a constant voltage (ConstV) of 0.5 V for 30 min.

2.3. Characterizations

The scanning electron microscope (SEM, JEOL JSM-820) equipped with the energy dispersive X-ray spectrometer (EDX) (Oxford INCA 7109) is used to examine the film morphology and composition. The X-ray diffraction (XRD) patterns are collected using an X-ray diffractometer (Rigaku SmartLab). The cyclic voltammetry (CV) measurements are conducted on the as-electrodeposited (not dealloyed) Ni–Cu films in the electrolyte used for electrodeposition and dealloying. The voltage is scanned between 0.5 V and −0.75 V at a rate of 50 mV s^{-1} with a potentiostat (PAR Verastat 3).

2.4. Electrodeposition of Ni^{III}O(OH)

Ni^{III}O(OH) is electrodeposited at 0.9 V in a solution of nickel (II) sulfate (0.5 M, Aldrich, ACS reagent) and ammonium hydroxide solution (0.5 M, Riedal–Dehaën, ACS reagent), following the previously reported method [25]. The amount of charge passed during the electrodeposition of Ni^{III}O(OH) is set at 0.2 C cm^{-2}. The actual mass of Ni^{III}O(OH) deposited is measured by an analytical balance (METTLER AT250 with the resolution of 0.01 mg and the readability (standard deviation) of 0.02 mg). After deposition, the sample is rinsed with deionized water and ethanol separately and then dried under N$_2$.

2.5. Electrochemical measurements for supercapacitor applications

Electrochemical measurements for supercapacitor applications are performed at room temperature with a potentiostat (PAR Verastat 3). A three-electrode system is used with the SCE as the reference electrode, a platinum foil (2 cm × 2 cm) as the counter electrode, and the sample as the working electrode. The electrolyte used is an aqueous solution of 1 M KOH. Cyclic voltammetry measurements are performed between −0.5 V and 0.5 V with a scan rate of 5 mV s^{-1}. Cyclic chronopotentiometric profiles are measured at a current density of 1.5, 3, 7.5, 15, 30 A g^{-1}, and the cycling stability is tested with a constant current density of 7.5 A g^{-1} for 1000 cycles.

3. Results and discussion

The voltage value of the pulsing steps is determined from the cyclic voltammogram measurement (Fig. S1) of the as-deposited Ni–Cu film: the pulse bias is set to be 0.06 V based on the observation that at 0.06 V a very low current was generated. Minimum current flow is desired for the pulsing steps in order to eliminate

metal dissolving or deposition during the pulsing steps, allowing "breaks" for the atom rearrangement to take place without disturbance. From the cyclic voltammogram measurement (Fig. S1), 0.5 V generates a reasonably high dealloying current, which is in good consistence with previous studies [10,11,19]. Thus, 0.5 V is chosen as the dealloying voltage for the high-voltage step.

Previous reports show that the presence of saccharin as a surfactant in the electroplating bath greatly affects the morphology of the deposited metal film, e.g., leading to greatly increased surface smoothness [23,24], however, the alloy films deposited with surfactants added are generally difficult to be dealloyed to form the desired nanoporous metallic structures, due to the fact that the surfactant molecules are likely to be trapped at the grain boundaries and can serve as barriers for the dealloying front to proceed, as indicated in the previous studies [19,20]. Here two groups of electroplating/dealloying experiments are carried out: one with saccharin in the electrolyte and the other without. The morphologies and compositions of the as-deposited and as-dealloyed films are shown in Fig. 1. It can be seen that the addition of saccharin leads to much smoother surface for the as-deposited Ni−Cu film (Figs. 1A and D), which is in good agreement with the previous studies [19,20].

It is evident, for the two groups of experiments (either with saccharin-free or saccharin-containing baths), porous structures with bigger pores, higher porosity, as well as thinner ligaments (Fig. 1C and F) are generated in the pulse-dealloyed samples compared with the ConstV-dealloyed ones (Fig. 1B and E). For example, for samples fabricated without the presence of saccharin, the ConstV-dealloyed Ni−Cu film exhibits pores of 50−200 nm, and ligaments of several hundred nanometers (Fig. 1B). By contrast, the pulse-dealloyed one shows bigger pores of 300−500 nm and much thinner ligaments, approximately 50 nm (Fig. 1C). Note that the calculated film porosities are also shown in Fig. 1. The film porosities are calculated by comparing the film compositions before and after dealloying, assuming that only Cu is removed during the dealloying process (see Supporting information). As a result, the pulse-dealloyed samples feature much higher porosity than the ConstV-dealloyed counterparts. Moreover, pulse dealloying generates porous Ni films with remarkably higher purities than ConstV-dealloying. For example, for samples prepared without saccharin, the Ni content of the pulse-dealloyed film is 87 wt.%, much higher

than 69 wt.% of the ConstV-dealloyed one. The higher Ni purity obtained in the pulse-dealloyed film is further confirmed by the XRD measurements (Fig. S2) which show that the (111) peak for the pulse-dealloyed film shifts to a higher diffraction angle which is closer to the (111) peak of pure Ni. The mechanism of the selective etching of Cu, the nobler component, was well studied by Searson and coworkers [19]. In brief, the formation of a passive oxide film on nickel in sulfamate solutions allows the selective electrochemical etching of Cu.

More interestingly, for samples prepared in the saccharin-containing bath, the film is barely dealloyed using the conventional ConstV method. This is evidenced by the film morphology of shallow and sparse small pores observed in SEM (Fig. 1E) and the barely varied Ni weight percentage of the treated film, indicating that the film prepared with saccharin has a much higher DT ($DT > 50$ wt.%, that is, >50 wt.% Cu required for dealloying to take place) than the one prepared without ($DT < 42$ wt.%). Again, this is because that the surfactant molecules in the electroplating solution may get trapped in the deposited film, particularly at the grain boundaries. During the dealloying process, the trapped surfactant molecules at the grain boundaries can serve as barriers to the migration of the metal atoms, retarding the dealloying process [19,20]. Moreover, it is found that this dealloying difficulty cannot be overcome by simply applying a higher dealloying voltage (e.g., 0.9 V), which only results in shallow and sparse pores (Fig. S3, see Supporting Information). Contrarily, pulse dealloying readily generates a porous structure (Fig. 1F) with significantly increased Ni purity (from 51 wt.% to 72 wt.%), illustrating the power and effectiveness of this novel dealloying method—particularly for significantly lowering DT.

As mentioned in Introduction, the dealloying process takes place in the following steps: 1) the reactive atoms are etched away at the alloy surface, 2) the inert atoms left at the alloy/electrolyte interface rearrange themselves and form clusters, exposing the reactive atoms underneath, 3) the newly exposed reactive atoms are etched, 4) Steps 2 and 3 are repeated until the dealloying front penetrates throughout the entire alloy material. Thus, the atomic rearrangement and chemical dissolution at the film/electrolyte interface determine the morphology and composition of the dealloyed materials finally obtained. The conventional dealloying method, either with a ConstV or no electric field applied, has little
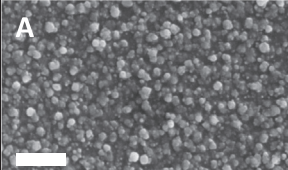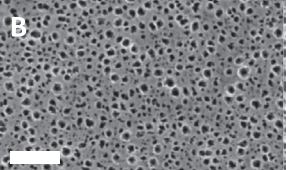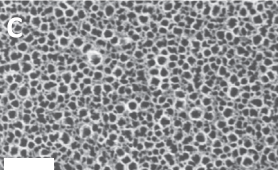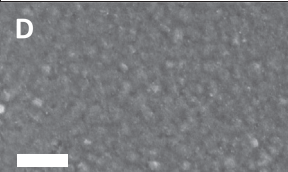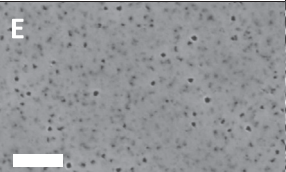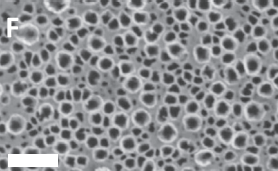

Dealloy voltage	Before dealloying	0.5 V	0.5 V (1 s) : 0.06 V (5 s)
W/O saccharin SEM	A	B	C
Ni wt.%	58	69	87
Porosity	−	16%	33%
W/ saccharin SEM	D	E	F
Ni wt.%	51	50	72
Porosity	−	0%	29%

Fig. 1. Plan-view SEM images, Ni contents, and porosities of the as-deposited and as-dealloyed (dealloyed for 30 min) Ni−Cu films. The scale bars indicate 2 μm.

control over the interaction between the atom rearrangement and chemical dissolution processes. For conventional dealloying, chemical dissolution strongly interferes with atomic rearrangement throughout the entire dealloying process. For example, as soon as the underlying reactive atoms are exposed, they undergo a dissolution reaction, which interferes with the previously ongoing atom rearrangement at the film/electrolyte interface. As a result, the voids created upon the dissolution of these reactive atoms may trigger new atom rearrangements locally; further disturbing the previously ongoing atom rearrangement. On the other hand, the insufficient atom rearrangement can in turn result in less exposure and dissolution of the more reactive atoms. Therefore, the conventional dealloying methods tend to render high DT/low purity/ low porosity samples, due to the incomplete atom rearrangement. On the contrary, the pulse dealloying method offers an effective control over the interaction between atom rearrangement and chemical dissolution, allowing more sufficient atom rearrangement by suppressing the chemical dissolution reaction frequently, so that the dealloyed materials with lower DT, higher purity, and higher porosity can be generated. Additionally, it should be noted that, compared with the conventional dealloying method, the pulse dealloying method allows for atom rearrangement at a larger scale and is likely to reduce the inhomogeneity in the pre-formed alloy materials. This effect can be clearly seen by comparing the ConstV- and pulse-dealloyed metallic multilayers (see Supporting info, Fig. S4). Ni—Cu multilayers with alternating compositions along the film thickness direction are first electrodeposited and then dealloyed. As illustrated, the pulse dealloying treatment preserves less the pre-built structural order in the Ni—Cu alloys than the ConstV-dealloying. Nevertheless, this "smoothing" effect of pulse dealloying can be beneficial in circumstances where a more homogeneous material is desired.

Consequently, considering that the chemical dissolution of metals (and thus the atom arrangement to some degree) can be controlled by tuning the voltage and duration of the bias applied, in principle, one can control the morphology and composition of the dealloyed metallic structure by tailoring the voltage profile applied. To verify this hypothesis, the impact of the time durations of the voltage steps, namely t_1 (at 0.5 V) and t_2 (at 0.06 V), of the pulsed voltage waveform on the dealloyed structure is investigated (Fig. 2). Compared with the voltage waveform with $t_1 = 1$ s and $t_2 = 5$ s (Fig. 2B), a less frequent pulsed waveform with $t_1 = 5$ s and $t_2 = 5$ s (Fig. 2A) leads to smaller pores, thicker ligament, smaller porosity, and lower Ni purity—in other words, the structure is more similar to the ConstV-dealloyed counterpart (Fig. 1B). Moreover, compared with voltage waveform with $t_1 = 1$ s and $t_2 = 5$ s (Fig. 2B), a longer pulsing step with $t_1 = 1$ s and $t_2 = 15$ s (Fig. 2C) leads to similar film porosity and Ni purity, but significantly smaller pores. Moreover, the overall dealloying time, $t_{dealloy}$, shows strong impact on the film morphology and composition (Fig. S5). By tuning the pulsed voltage

profiles, various porous morphologies and film compositions are achieved, illustrating the great flexibility of the pulse dealloying method for convenient structural control. The nanoporous Ni films fabricated by the pulse dealloying method are tested in supercapacitor applications. Because of their wide range of potential applications, supercapacitors as a type of charge storage device have been intensively investigated. To achieve high-performance supercapacitors, a strategy attracted much attention lately is to coat the electro-active materials on conductive host frameworks in order to 1) more efficiently utilize the electro-active materials by providing a much enlarged working surface area 2) dramatically lower the internal resistance by enabling direct charge transfer from the usually poorly conductive electro-active materials to the charge collectors (i.e., the conductive frameworks) [3–5,11,26,27]. The conductive frameworks used for supercapacitor electrodes (e.g. nanoporous Au) are commonly fabricated using the dealloying techniques [5,11].

Here, we compare pulse-dealloyed and ConstV-dealloyed porous Ni for the supercapacitor applications. The dealloyed Ni frameworks (∼700 nm thick) are first electrochemically deposited with a thin layer of $Ni^{III}O(OH)$ and then tested as the supercapacitor electrodes. The weight of $Ni^{III}O(OH)$ deposited is determined by the gravimetric method and measured to be 0.127 mg cm^{-2}. The top-view SEM measurements reveal that the pores were neither clogged nor dramatically shrunk upon coated with $Ni^{III}O(OH)$ for both types of electrodes (Fig. 3A). The cyclic voltammetry curve (Fig. 3B) of the electrode based on pulse-dealloyed Ni possesses a larger enclosed area than the one on ConstV-dealloyed Ni, indicating an improved capacitive property of the former. Chronopotentiometric measurements at a discharge current density of 1.5 A g^{-1} (Fig. 3C) show that the electrode based on the pulse-dealloyed Ni framework possesses much longer discharging time and therefore a significantly larger SC (1521 F g^{-1}) than the one based on the ConstV-dealloyed Ni structure (1032 F g^{-1}), which is calculated with the following equation (Eq. (1)):

$$C_{m} = \frac{I\Delta t}{m\Delta V} \tag{1}$$

where C_m is the specific capacitance (SC) of the electrode, I the galvanic discharge current, Δt the full discharge time, m the mass of the electroactive material, and ΔV the potential window.

The chronopotentiometric profiles are further investigated at different charge/discharge current densities (Fig. 3D and E). The SCs of $Ni^{III}O(OH)$ deposited on the pulse-dealloyed/ConstV-dealloyed Ni films are measured to be 1521/1032, 1479/993, 1446/929, 1393/893, 1288/857 F g^{-1} at 1.5, 3, 7.5, 15, and 30 A g^{-1}, respectively. The significant improvement in SC further indicates the pulse-dealloyed films possess larger surface area than the ConstV-dealloyed ones. This is because charge in a supercapacitor is
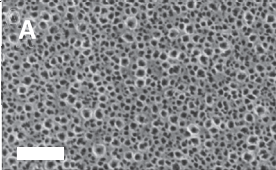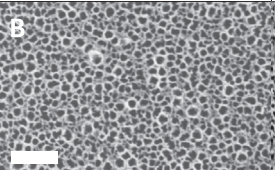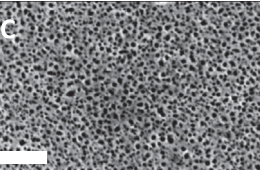

	Dealloy voltage	0.5 V (5 s) : 0.06 V (5 s)	0.5 V (1 s) : 0.06 V (5 s)	0.5 V (1 s) : 0.06 V (15 s)
W/O saccharin	SEM	A	B	C
	Ni wt.%	75	87	84
	Porosity	23%	33%	31%

Fig. 2. Plane-view SEM images, Ni contents, and porosities of the pulse-dealloyed films fabricated with different t_1 and t_2 (films prepared without the addition of saccharin in the electrolyte, dealloyed for 30 min). The scale bars indicate 2 μm.
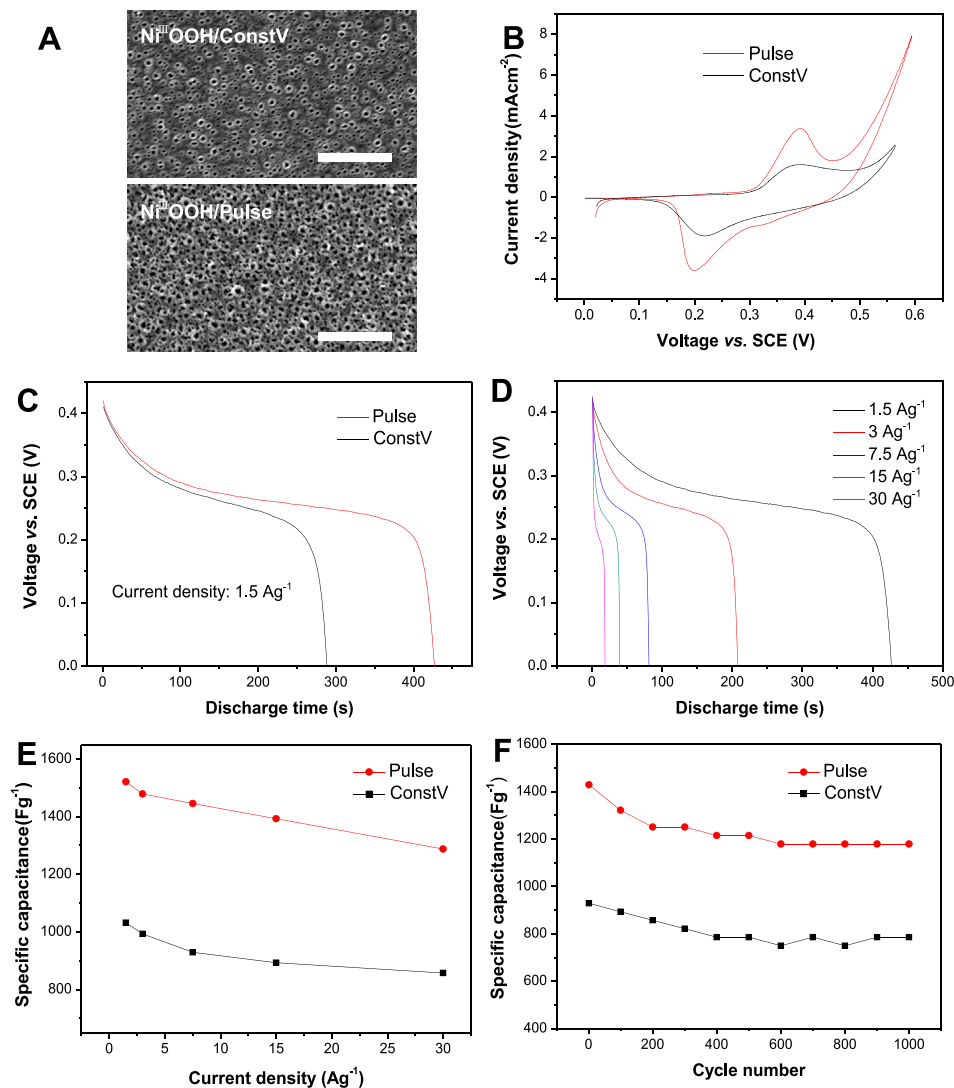
Fig. 3. Surface morphologies and electrochemical capacitance performance of $Ni^{III}O(OH)$ coated on the ConstV-dealloyed and pulse-dealloyed Ni scaffolds: A) Top-view SEM images. The scale bars indicate 5 μm. B) cyclic voltammogram curves with a scan rate of 5 mV s^{-1}. C) Chronopotentiometric curves at a constant charge/discharge current density of 1.5 A g^{-1}. D) Chronopotentiometric curves at different current densities for $Ni^{III}O(OH)$ coated on the pulse-dealloyed Ni framework. E) SCs at different current densities. F) Cycling performance at 7.5 A g^{-1}.

generally stored through electrochemical reactions within a very shallow skin depth (usually within several nm) of the electro-active materials [28], thus the mass-specific capacitance of an electro-active material can be a direct indicator of its specific surface area. On the other hand, the gradual SC decrease with increasing charge/discharge rate observed on both types of electrodes (Fig. 3D and E) can be ascribed to the diffusion-controlled nature of the redox reaction (Eq. (2)) that takes place mainly at the surfaces of the electro-active materials [29,30].

$$Ni^{II}(OH)_2 + OH^- \rightarrow Ni^{III}O(OH) + H_2O + e^- \qquad (2)$$
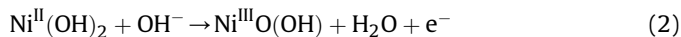
The cycling performance for both types of electrode is tested at 7.5 A g^{-1} for 1000 cycles (Fig. 3F). Having a more porous structure with finer ligaments, the pulse-constructed electrode displayed the similar cycling stability as the ConstV-constructed one. The SC of the pulse-constructed electrode decreases ∼15% in the first 200 cycles and then gradually levels off with no further deprecation in the last 400 cycles, while the SC of the ConstV-constructed electrode drops ∼18% in the first 400 cycles before entering a stabilized level.

It should be pointed out [5,11,31–36] that nickel oxides have been widely studied for supercapacitor electrodes. The application of conductive frameworks to host nickel oxides has proved to be particularly effective for improving their performance. For example, macroscopic Ni foams with sub-mm pores [31,33], Ni nanoparticles [32], conventionally dealloyed metals [5], nanoporous Ni frameworks with corrugated pore walls [11], and graphene [36] have been reported as effective conductive frameworks. The pulse-dealloyed Ni framework reported in this study serves as a novel type of low-cost conductive host framework for supercapacitor electrodes that enables high electrochemical performance comparable to the best ones reported to date.

4. Conclusion

In summary, we demonstrate a novel electrochemical dealloying method using pulsed voltage profiles for conveniently controlling the morphology and composition in the porous metal product. This dealloying method proves to be particularly powerful in allowing the dealloying reaction to take place at a significantly

lower composition of the more reactive metal component and in achieving a more thorough dealloying to yield a porous metal product of higher purity. Moreover, thinner ligaments and larger specific surface area can be generated. Compared with the conventionally dealloyed porous metals, the porous metals enabled by the method reported here can be well-suited for the wide-ranging applications (such as catalysts, supercapacitor/battery electrodes, and sensors) that call for higher purities, finer porous morphologies, or larger specific surface areas in nanoporous metallic materials.

Acknowledgments

Appendix A. Supplementary data

Supplementary data related to this article can be found at http://dx.doi.org/10.1016/j.jpowsour.2013.11.039.

References

[1] Y. Ding, Y.J. Kim, J. Erlebacher, Adv. Mater. 16 (2004) 1897–1900.
[2] F.L. Jia, C.F. Yu, K.J. Deng, L.Z. Zhang, J. Phys. Chem. C 111 (2007) 8424–8431.
[3] A.S. Arico, P. Bruce, B. Scrosati, J.M. Tarascon, W. van Schalkwijk, Nat. Mater. 4 (2005) 366–377.
[4] J.L. Kang, L.Y. Chen, Y. Hou, C. Li, T. Fujita, X.Y. Lang, A. Hirata, M.W. Chen, Adv. Energy Mater. 3 (2013) 857–863.
[5] X.Y. Lang, A. Hirata, T. Fujita, M.W. Chen, Nat. Nanotechnol. 6 (2011) 232–236.
[6] D.S. Kong, J.M. Wang, H.B. Shao, J.Q. Zhang, C.N. Cao, J. Alloys Compd. 509 (2011) 5611–5616.
[7] J.H. Pikul, H.G. Zhang, J. Cho, P.V. Braun, W.P. King, Nat. Commun. 4 (2013) 1732.
[8] L. Zhang, H. Chang, A. Hirata, H. Wu, Q.-K. Xue, M. Chen, ACS Nano 7 (2013) 4595–4600.
[9] M. Yan, T. Jin, Q. Chen, H.E. Ho, T. Fujita, L.Y. Chen, M. Bao, M.W. Chen, N. Asao, Y. Yamamoto, Org. Lett. 15 (2013) 1484–1487.
[10] C.K. Tsang, Z. Xu, Y.Y. Li, J. Electrochem. Soc. 156 (2009) D508.
[11] C.K. Tsang, S.S. Zeng, H. Cheng, L.X. Zheng, J. Zhang, H. Li, S.W. Shu, T.F. Hung, J. Lu, Y.Y. Li, Energy Technol. 1 (2013) 478–483.
[12] L. Liu, W. Lee, Z. Huang, R. Scholz, U. Gösele, Nanotechnology 19 (2008) 335604.
[13] L. Liu, E. Pippel, R. Scholz, U. Gösele, Nano Lett. 9 (2009) 4352–4358.
[14] L. Liu, R. Scholz, E. Pippel, U. Gosele, J. Mater. Chem. 20 (2010) 5621–5627.
[15] J. Cai, J. Xu, J.M. Wang, L.Y. Zhang, H. Zhou, Y. Zhong, D. Chen, H.Q. Fan, H.B. Shao, J.Q. Zhang, C.N. Cao, Int. J. Hydrogen Energy 38 (2013) 934–941.
[16] Y.N. Li, Z.P. Xi, X.T. Kang, H.P. Tang, W.Y. Zhang, J. Zhang, G.Z. Li, Intermetallics 17 (2009) 1065–1069.
[17] Y.L.H. Lu, F. Wang, Scripta Mater. 56 (2007) 165.
[18] N.A. Senior, R.C. Newman, Nanotechnology 17 (2006) 2311–2316.
[19] L. Sun, C.L. Chien, P.C. Searson, Chem. Mater. 16 (2004) 3125–3129.
[20] S. Cherevko, N. Kulyk, C.H. Chung, Nanoscale 4 (2012) 568–575.
[21] L.H. Qian, M.W. Chen, Appl. Phys. Lett. 91 (2007) 083105.
[22] J. Erlebacher, M.J. Aziz, A. Karma, N. Dimitrov, K. Sieradzki, Nature 410 (2001) 450–453.
[23] J.C. Hsu, K.L. Lin, Thin Solid Films 471 (2005) 186–193.
[24] A.M. Rashidi, A. Amadeh, Surf. Coat. Technol. 204 (2009) 353–358.
[25] A.J. Varkey, A.F. Fort, Thin Solid Films 235 (1993) 47–50.
[26] J.H. Kim, S.H. Kang, K. Zhu, J.Y. Kim, N.R. Neale, A.J. Frank, Chem. Commun. 47 (2011) 5214.
[27] M.J. Deng, C.Z. Song, P.J. Ho, C.C. Wang, J.M. Chen, K.T. Lu, Phys. Chem. Chem. Phys. 15 (2013) 7479.
[28] P. Simon, Y. Gogotsi, Nat. Mater. 7 (2008) 845–854.
[29] Z. Mao, P. De Vidts, R.E. White, J. Newman, J. Electrochem. Soc. 141 (1994) 54–64.
[30] C. Lin, B.N. Popov, H.J. Ploehn, J. Electrochem. Soc. 149 (2002) A167–A175.
[31] G.W. Yang, C.L. Xu, H.L. Li, Chem. Commun. (2008) 6537–6539.
[32] Q. Lu, M.W. Lattanzi, Y. Chen, X. Kou, W. Li, X. Fan, K.M. Unruh, J.G. Chen, J.Q. Xiao, Angew. Chem. Int. Ed. 50 (2011) 6847–6850.
[33] Z. Lu, Z. Chang, J. Liu, X. Sun, Nano Res. 4 (2011) 658–665.
[34] H. Pang, B. Zhang, J. Du, J. Chen, J. Zhang, S. Li, RSC Adv. 2 (2012) 2257–2261.
[35] X. Xia, J. Tu, Y. Zhang, X. Wang, C. Gu, X.-b. Zhao, H.J. Fan, ACS Nano 6 (2012) 5531–5538.
[36] J. Yan, Z. Fan, W. Sun, G. Ning, T. Wei, Q. Zhang, R. Zhang, L. Zhi, F. Wei, Adv. Funct. Mater. 22 (2012) 2632–2641.